https://doi.org/10.5194/nhess-2022-114
Preprint. Discussion started: 31 March 2022

Natural Hazards and Earth System Sciences
Discussions

Spatiotemporial seismicity pattern of the Taiwan orogen

Yi-Ying Wen[1, 2*], Chien-Chih Chen[3, 4], Strong Wen[1, 2], and Wei-Tsen Lu[1]

[1]Department of Earth and Environmental Sciences, National Chung Cheng University, Chia-yi County 62102, Taiwan
[2]Environment and Disaster Monitoring Center, National Chung Cheng University, Chia-yi County 62102, Taiwan
[3]Department of Earth Sciences, National Central University, Taoyuan City 32001, Taiwan
[4]Earthquake-Disaster & Risk Evaluation and Management Center, National Central University, Taoyuan City 32001, Taiwan

Correspondence: Yi-Ying Wen (yiyingwen@ccu.edu.tw)

Abstract

We investigate the temporal and spatial seismicity patterns prior to eight M>6 events nucleating in different region of Taiwan through region-time-length algorithm and analysis of self-organizing spinodal model. Our results reveal that the spatiotemporial seismicity variations during the preparation process of impending earthquakes would display distinctive pattern corresponding to the tectonic setting. Q-type events occur in southern Taiwan and experience seismic quiescence stage prior to the mainshock. Seismicity decrease of 2.5<M<4.5 events around the high b-value southern Central Range, which contributes to accumulate the tectonic stress for preparing the occurrence of the Q-type event. On the other hand, A-type events occur in central Taiwan and experience seismic activation stage prior to the mainshock, which nucleated on the edge of the seismic activation area. We should pay attention when accelerating seismicity of 3<M<5 events appears within the low b-value area, which would promote the nucleation process of the A-type event.

https://doi.org/10.5194/nhess-2022-114
Preprint. Discussion started: 31 March 2022


Natural Hazards and Earth System Sciences
Discussions

1. Introduction

Seismic activity is related to spatiotemporal variation of stress field and state, and seismicity changes prior to a large earthquake have been widely observed through different techniques, e.g., b-values (Chan et al., 2012; Wyss and Stefansson, 2006), PAST (Mignan and Giovambattista, 2008), PI (Rundle et al., 2003; Chen et al., 2005), and RTL (Chen and Wu, 2006; Wen et al., 2016). Previous studies most focus on a significant earthquake, therefore it is not easy to understand whether the properties of seismic activation and quiescence pattern respond with the regional tectonic stress.

The Taiwan orogenic belt, which is an active and ongoing arc-continent collision zone as a result of the Philippine Sea Plate (PSP) oblique colliding with the Eurasian Plate (EP), is particularly complex due to the two adjacent subduction zones, the Ryukyu trench and the Manila trench in the northeast and south of island, respectively (Suppe, 1984; Yu et al., 1997). The frequent and significant seismic activities as well as the rapid convergence rate of 85 to 90 mm/yr are well observed by the island-wide GPS and seismic networks (Fig. 1). Suppe (1984) pointed out that the growth of Taiwan orogenic belt shows propagation from north to south due to the oblique plate convergence and the opposing subduction in the southern and northern parts of Taiwan. In the southern Taiwan, the EP subducting eastward beneath the PSP is in the stage of incipient arc-continent collision (Kao et al., 2000; Shyu et al., 2005). The coastal plain and foothill region, which represent the southern tip of the fold-and-thrust belt in the western Taiwan and show very low seismicity, mainly consist of the Miocene shallow marine deposits and the Plio-Pleistocene foreland basin as well as mudstones. On the other hand, the southern Central Range is mainly composed of Oligocence to Miocence metamorphic slates and comprises ductile folds and cleavages as well as superimposed faults. The central Taiwan, which is considered as the rapid to full collision, mainly

https://doi.org/10.5194/nhess-2022-114
Preprint. Discussion started: 31 March 2022

Natural Hazards and Earth System Sciences
Discussions

consists of Coastal Range, Central Range and Western Foothills (Shyu et al., 2005). A myriad of active and thin-skinned structures are the products of the accretion of the continental sliver to the continental margin. Over the last two decades, several moderate earthquakes occurred in the various seismicity pattern and GPS velocity field regions. This give us a chance to further investigate the spatiotemporal seismic pattern related to the regional tectonic stress.

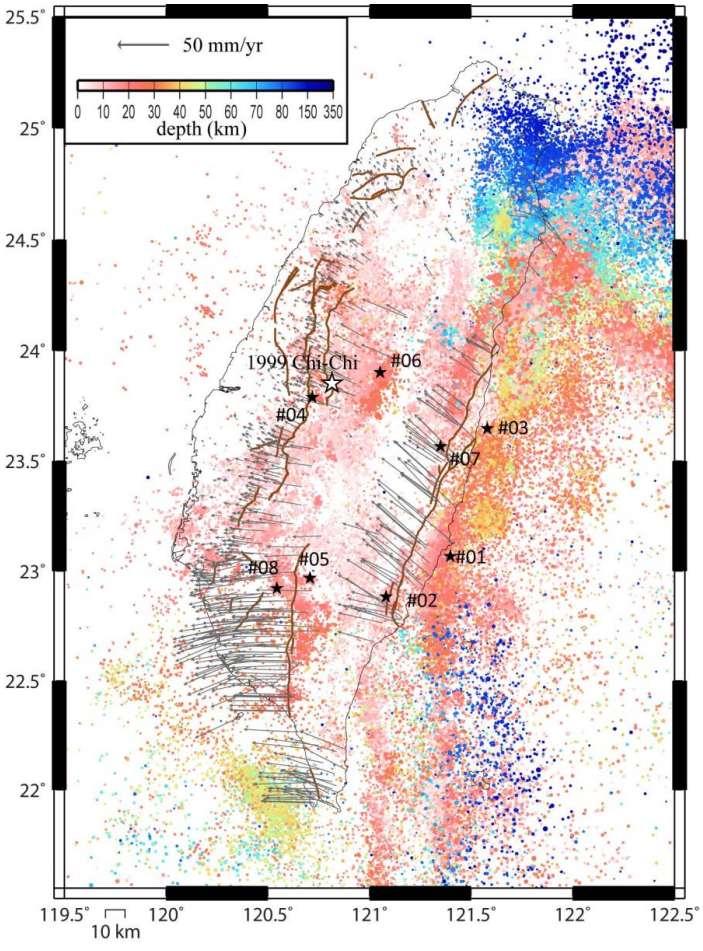

Figure 1: Horizontal velocities from 2002 to 2017 (Chen et al., 2018) and seismicity between 1991 to 2018. The white star shows the location of 1999 Chi-Chi earthquake, and the black stars represent the locations of the investigated events in this study. The active faults (thick lines) identified by the Central Geological Survey of Taiwan are also shown.

https://doi.org/10.5194/nhess-2022-114
Preprint. Discussion started: 31 March 2022


Natural Hazards and Earth System Sciences
Discussions

2. RTL Algorithm and Data

The region-time-length (RTL) algorithm (Sobolev and Tyupkin, 1997; 1999) is a statistical technique to detect the occurrence of seismic quiescence and activation by taking account of location, occurrence time and magnitude of earthquakes. The RTL value is defined as the product of the three dimensionless factors, *R*, *T* and *L*:

$$R(x,y,z,t) = \left[\sum_{i=1}^{n} \exp\left(-\frac{r_i}{r_0}\right)\right] - R_{bk}(x,y,z,t) \quad (1)$$

$$T(x,y,z,t) = \left[\sum_{i=1}^{n} \exp\left(-\frac{t-t_i}{t_0}\right)\right] - T_{bk}(x,y,z,t) \quad (2)$$

$$L(x,y,z,t) = \left[\sum_{i=1}^{n} \left(\frac{l_i}{r_i}\right)\right] - L_{bk}(x,y,z,t) \quad (3)$$

where r_i is the distance between the investigated point (x, y, z) and the ith prior event (with the occurrence time t_i and rupture length l_i). n is the number of prior events occurred in a defined space-time window with $r_i \leq 2r_0$ (r_0, characteristic distance) and $(t - t_i) \leq 2t_0$ (t_0, characteristic time-span). Rupture length l_i is the function of earthquake magnitude (M_i), $\log l_i = 0.5M_i - 1.8$ (Kasahara, 1981). The weighted RTL value reflects the deviation from the background seismicity level (R_{bk}, T_{bk} and L_{bk}) with negative value for seismic quiescence and positive value for an activation, respectively. Here, we adopt the r_0= 47.5 km and t_0= 1.15 yr model parameters based on previous studies for Taiwan (Chen and Wu, 2006; Wen et al., 2016; Lu, 2017; Wen and Chen, 2017).

For statistical analyses, the catalog completeness is the most important factor. Since 1991, the Taiwan Telemetered Seismographic Network (TTSN) (Wang, 1989) merged to the Central Weather Bureau (CWB) seismic network and updated to an integrated earthquake observation system, named Central Weather Bureau Seismic Network (CWBSN). Wang et al. (1994) pointed out that most of shallow earthquakes occurring in Taiwan distributed in the depth range less than 35 km. We used the

https://doi.org/10.5194/nhess-2022-114
Preprint. Discussion started: 31 March 2022

Natural Hazards and Earth System Sciences
Discussions

earthquake catalogue maintained by CWB for the entire Taiwan area with M≥2.5 and depth≤35 km between 1991 to 2018 and applied a declustering procedure proposed by Gardner and Knopoff (1974). Considering the sufficient background seismicity and minimizing the influence of the 1999 Chi-Chi earthquake, we only selected the M>6 inland earthquakes between 2003 and 2016 in Taiwan. Since two events occurred in a close space-time window would show high similarity in RTL function (Lu, 2017), we neglected the event occurred within $2t_0$ and r_0 with respect to the last M>6 events. For example, two M>6 events within a distance of 10 km struck the Nantou area on 27 March 2013 and 02 June 2013, we only analyzed the former event. Therefore, we have eight qualified M>6 events, as list in Table 1.

Table 1: Earthquake parameters for the investigated events determined by CWB.

No.	Date (UT)	Long. (deg.)	Lat. (deg.)	Depth (km)	M_L
1	2003/12/10 04:38:14	121.398	23.067	17.7	6.4
2	2006/04/01 10:02:20	121.081	22.884	7.2	6.2
3	2009/10/03 17:36:06	121.579	23.648	29.2	6.1
4	2009/11/05 09:32:58	120.719	23.789	24.1	6.2
5	2010/03/04 00:18:52	120.707	22.969	22.6	6.4
6	2013/03/27 02:03:20	121.053	23.902	19.4	6.1
7	2013/10/31 12:02:10	121.349	23.566	15.0	6.4
8	2016/02/05 19:57:26	120.544	22.922	14.6	6.6

3. Results

https://doi.org/10.5194/nhess-2022-114
Preprint. Discussion started: 31 March 2022

Natural Hazards and Earth System Sciences
Discussions

3.1 Temporal Seismicity variation

The temporal variation in the RTL function represents the different stage of seismicity rate change at the target location with respect to the background level. For the consistency, we adopt 10-year catalogue as background for each investigated event. Figure 2 shows the temporal variation of the RTL functions prior to the investigated events. We can see that, before the occurrence of the investigated event, both seismicity changes are observed: seismic quiescence stage for Nos. 1, 2, 5 and 8 (Q-type events hereafter); seismic activation stage for Nos. 3, 4, 6 and 7 (A-type events hereafter), respectively. Q-type events occurred on different locations in southern Taiwan, and most, 3 among 4, of their temporal RTL functions reveal the seismic quiescence stages during 2002-2004, which is before the occurrence of 2003 Chengkung earthquakes. The

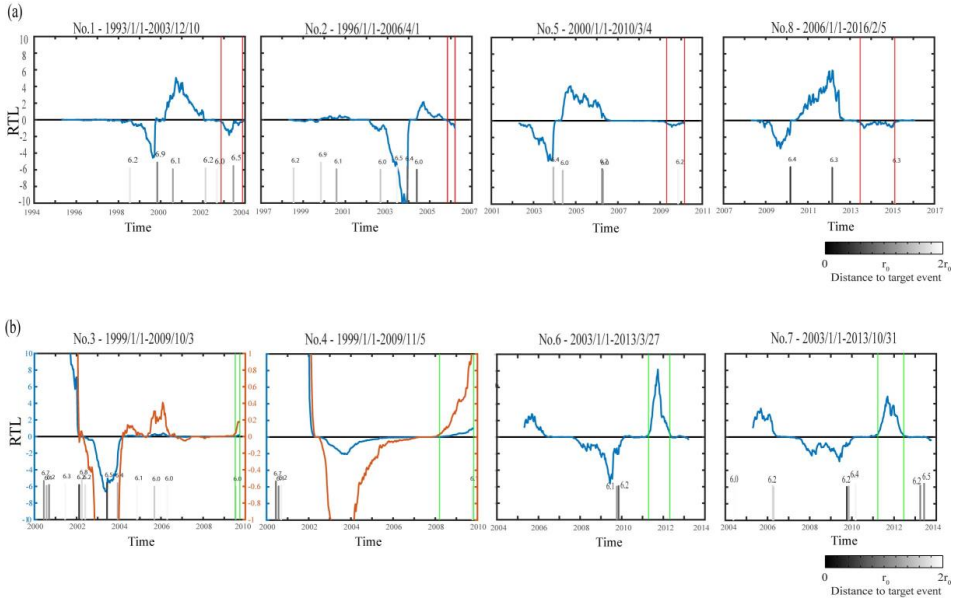

Figure 2: Temporal variation of the RTL function (blue line) for (a) Q-type events and (b) A-type events. The vertical red lines mark the seismic quiescence stage, and the vertical green mark the seismic activation stage. The bar chart represents the occurrence time of $M \geq 6.0$ events within the distance of $2r_0$ from the target event; each number above the bar is the magnitude.

https://doi.org/10.5194/nhess-2022-114
Preprint. Discussion started: 31 March 2022

Natural Hazards and Earth System Sciences
Discussions

seismicity increase (activation stage) took about two years following the 2003 Chengkung mainshock, i.e., event No. 1. We notice that the length of seismic quiescence stage prior to the Q-type event might correspond to the magnitude. A-type events all occurred in central Taiwan and located within $2r_0$ with respect to the 1999 Chi-Chi earthquake. Figure 3 shows the declustered seismicity distribution as a function of time and latitude. It is noticed that the significant seismicity following the 1999 Chi-Chi earthquake in the north of 23°N. Since the background seismicity of event Nos. 3 and 4 starting from 1999/01/01, the RTL functions are obviously affected by the occurrence of the 1999 Chi-Chi earthquake. Therefore, we enlarge the vertical axis to

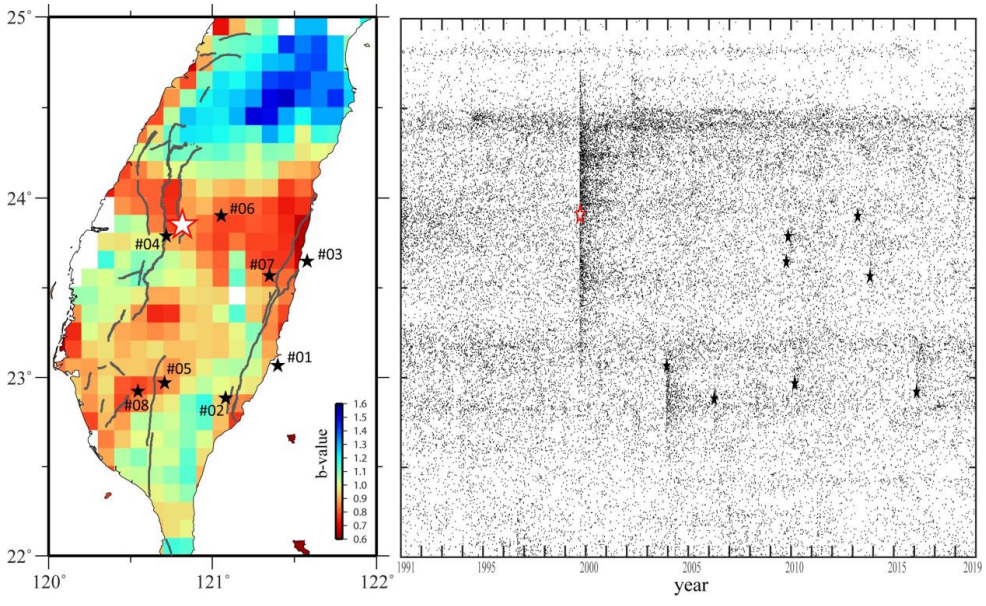

Figure 3: Map view of earthquake b-value and declustered seismicity distribution as a function of time and latitude. The white star indicates the 1999 Chi-Chi earthquake, and the black stars represent the investigated events in this study. The active faults (thick lines) identified by the Central Geological Survey of Taiwan are also shown.

accentuate the seismicity variation prior to event Nos. 3 and 4. As shown in Fig. 2, the temporal RTL functions of A-type events most show seismic activation stage between

https://doi.org/10.5194/nhess-2022-114
Preprint. Discussion started: 31 March 2022


Natural Hazards and Earth System Sciences
Discussions

2004-2006, which correspond to the seismicity increase following the 2003 Chengkung mainshock. However, for the A-type event, we could not see the relationship between the length of seismic activation stage and the magnitude.

3.2 Spatial Seismic Activation/Quiescence Distribution

Since Q-type and A-type events located in southern and central Taiwan, respectively, it would be worth to examine the spatial pattern of their abnormal seismicity stages. Wen and Chen (2017) pointed out that various seismic activation or quiescence processes of about 2-4 years were found prior to some events occurred in Taiwan. Thus, for the consistency, we select the last abnormal stage within four years prior to the investigated events, as marked by red vertical lines for quiescence stage of Q-type events and green vertical lines for activation stage of A-type events, respectively. Then, we calculate the summation of selected period to generate the seismic quiescence/activation distribution. Considering the definition of the weighted RTL function, the sufficient number of background seismicity should be regarded as a criterion. Using the declustered catalogue during 1991 to 2016, we set up two conditions for each grid to strengthen the reliability: (i) the total number of events within the grid area of 0.1°×0.1° must be more than 26 (i.e., at least 1 event occurred every year on average); (ii) the total events within a circle of $2r_0$ in radius must be more than 9360 (i.e., at least 30 events occurred every month on average). Similar with previous studies (e.g., Huang et al., 2001; Huang and Ding, 2012), Figure 4 shows that Q-type events occurred on the edge of the seismic quiescence area and A-type events occurred on the edge of the seismic activation area.

https://doi.org/10.5194/nhess-2022-114
Preprint. Discussion started: 31 March 2022

Natural Hazards and Earth System Sciences
Discussions

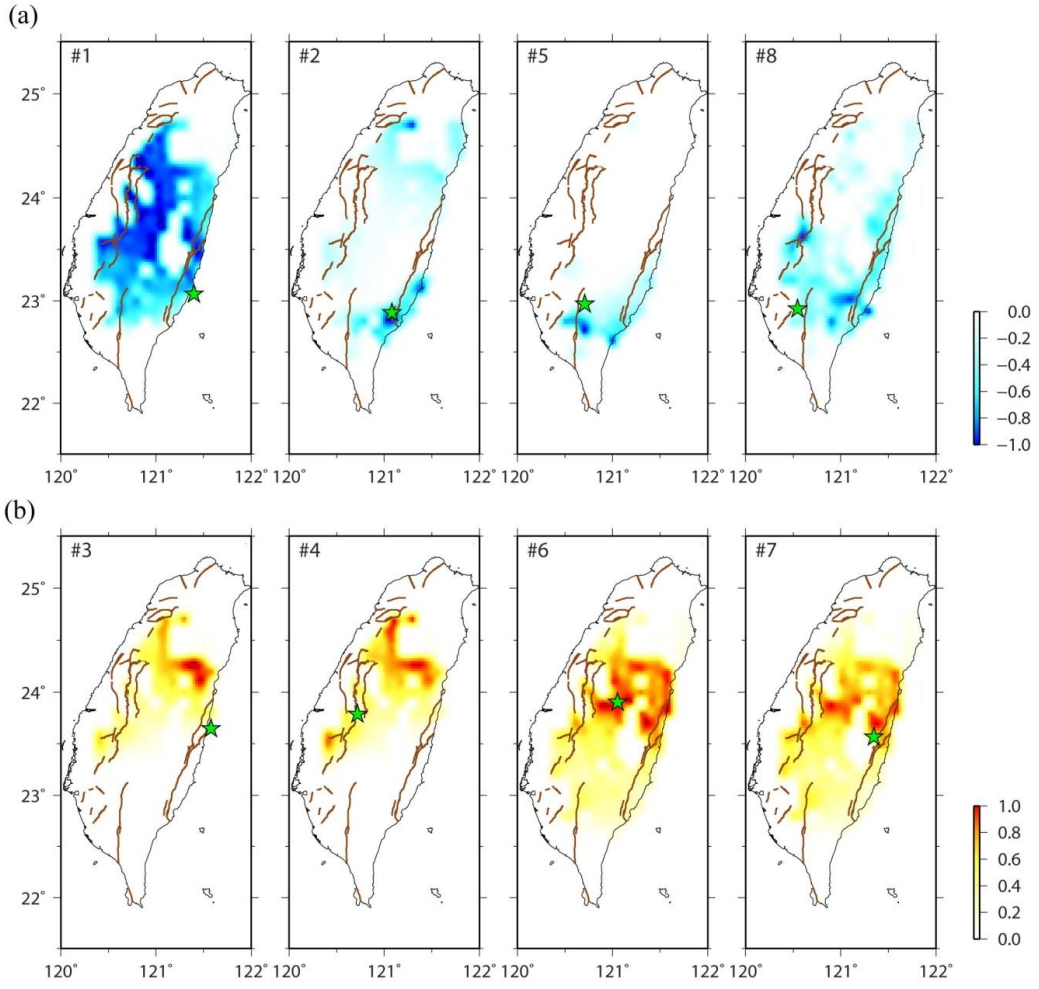

Figure 4: (a) The summed seismic quiescence map for the selected time window of the temporal RTL function of Q-type events, and (b) the summed seismic activation map for the selected time window of the temporal RTL function of A-type events. Stars represent the locations of the investigated events. The active faults (thick lines) identified by the Central Geological Survey of Taiwan are also shown.

4. Discussion

4.1 Spatiotemporal Characteristics of Seismicity Changes

The RTL analysis accounts for the background seismicity prior to the investigated event. For example, the analysis for event No. 1 (i.e., 2003 Chengkung earthquake)

https://doi.org/10.5194/nhess-2022-114
Preprint. Discussion started: 31 March 2022


Natural Hazards and Earth System Sciences
Discussions

used the declustered catalogue between 1993/01/01 to 2003/12/09 as background seismicity for each grid. It is noticed that four A-type events occurred in two different years: event Nos. 3 and 4 in 2009, as well as event Nos. 6 and 7 in 2013 (Fig. 2). Therefore, the RTL analyses account for almost the same background length for event Nos. 3 and 4 as well as for event Nos. 6 and 7, respectively. As the temporal RTL functions show the seismic activation stage prior to the mainshocks during the similar period, we could expect the similar seismic activation maps, as shown in Fig. 4. Furthermore, the seismic quiescence stage of event No. 5 occurred in the similar period of the seismic activation stage of event No. 3 (Fig. 2), and the seismic quiescence area of event No. 5 plays as a complement to seismic activation area of event No. 3 (Fig. 4). On the contrary, although event Nos. 3 and 7 occurred on the close locations, the difference of 4-year background seismicity affects the weighting of the deviation. For example, as shown in Fig. 2, the seismic quiescence stage during 2007-2009 revealed in the temporal RTL function of event No. 7 is evaluated as the background seismicity level in the temporal RTL function with respect to event No. 3. On the other hand, Wen and Chen (2017) pointed out that an abnormal seismic stage revealed with various background period cannot be produced by chance. The temporal RTL functions of five events (Nos. 1-5 in Fig. 2) accounting for different background periods all reveal the seismic quiescence stage before the occurrence of event No. 1. This phenomenon is consistent with the seismic quiescence map of event No. 1 (Fig. 4) and Z-value map of Wu et al. (2008) that, the seismicity activity decreased during 2002-2003 for large area in Taiwan. In addition, the widespread seismic activation distribution of Nos. 6 and 7 (Fig. 4) also respond to the seismicity activity increasing during 2011-2012 (Nos. 6-8 in Fig. 2). Overall, the seismic quiescence and activation maps show some characteristics: (i) the seismicity decrease is revealed in the southern Central Range

https://doi.org/10.5194/nhess-2022-114
Preprint. Discussion started: 31 March 2022


Natural Hazards and Earth System Sciences
Discussions

prior to the Q-type mainshocks; (ii) it seems the boundaries around 23.2°N and 24.5°N for the abnormal seismicity distributions, which coincide with the distribution of declustered seismicity in Fig. 3.

Rundle et al. (2000) proposed the self-organizing spinodal (SOS) model for characteristic earthquakes and suggested that small earthquakes occurred uniformly at all times while occurrence rate of the intermediate-sized earthquakes varied during the earthquake cycle. Chen (2003) investigated the SOS behavior of the 1999 Chi-Chi earthquake and revealed the seismic activation of moderate-size ($5<M<6$) events prior to the mainshock. Here, we also calculate the cumulative frequency-magnitude distributions for these eight events, using the same catalog periods of the RTL analysis. For each investigated event, we only compared the distribution diagrams of long-term (background period) and abnormal seismic stage marked in Fig. 2, within a radius of 25 km with respect to the epicenter. As shown in Fig. 5, cumulative frequency-magnitude distributions of long-term seismicity (red dots) generally exhibit linear power law distributions. For the Q-type events, the cumulative frequency distributions of seismic quiescence stage (black dots) appear lack in number of $2.5<M<4.5$ events (Fig. 5a), and the lacking level corresponds to the seismic quiescence distribution near the epicenter (Fig. 4). This indicates that, within the seismic quiescence stage before the occurrence of Q-type event, the quiescence of $2.5<M<4.5$ activity contributes to the accumulation of tectonic stress. On the other hand, the cumulative frequency distributions of seismic activation stage of the A-type events (black dots in Fig. 5b) display that the seismic activation of $3<M<5$ events within the seismic activation stage before the occurrence of A-type earthquake can be found, and this is similar with the result of the 1999 Chi-Chi earthquake (Chen, 2003). Event Nos. 6 and 7, which locate

https://doi.org/10.5194/nhess-2022-114
Preprint. Discussion started: 31 March 2022

Natural Hazards and Earth System Sciences
Discussions

very close to the high seismic activation area (Fig. 4), display obvious increase in number of 4<M<5 events during the seismic activation stage (Fig. 5b).

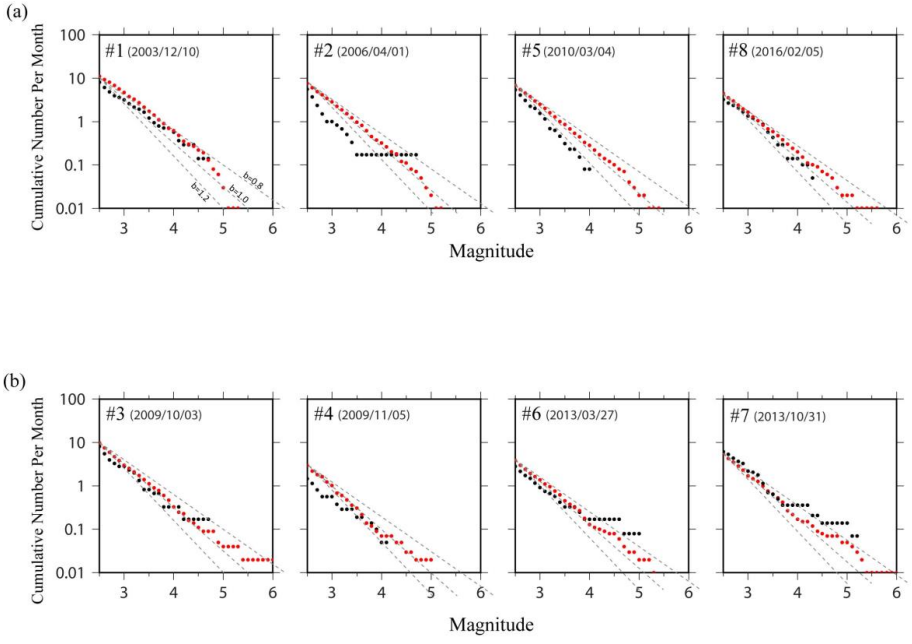

Figure 5: The cumulative frequency-magnitude distributions prior to the investigated events. Red and black dots represent the long-term and abnormal seismic stage marked in Fig. 2, respectively.

Event No. 4 occurs only one month later than event No. 3, however, the seismic activation stage of event No. 4 is much longer than that of event No. 3. Furthermore, the cumulative frequency distributions of seismic activation stage of event No. 4 display the lower intercept, which represents the overall decreasing seismicity within this seismic activation stage (Fig. 5b). Here, we further divide the seismic activation stage of event No. 4 into three periods for discussion: (i) P1: 2008/02-2009/03 before the seismic activation stage of event No. 3; (ii) P2: 2009/04-2009/09 matching the seismic activation stage of event No. 4; and (iii) P3: 2009/10 between the occurrences of event Nos. 3 and 4. The seismic activation distributions in Fig. 6 are all normalized with respect to the maximum RTL value of seismic activation distribution of event No. 4.

https://doi.org/10.5194/nhess-2022-114
Preprint. Discussion started: 31 March 2022

Natural Hazards and Earth System Sciences
Discussions

We can see that, before the seismic activation stage of event No. 3 during 2008/02-2009/03 (P1), the location of event No. 3 indeed shows no seismic activation, as revealing in the temporal RTL function (Fig. 2b). On the other hand, for the location of event No. 4, the seismic activation remains through all three periods P1-P3. Combining with the overall decreasing seismicity indicated by the lower intercept in Fig. 5(b), it suggests that this seismic activation prior to event No. 4 is mainly contributed by the relatively accelerating activity of 3.5<M<4 events.

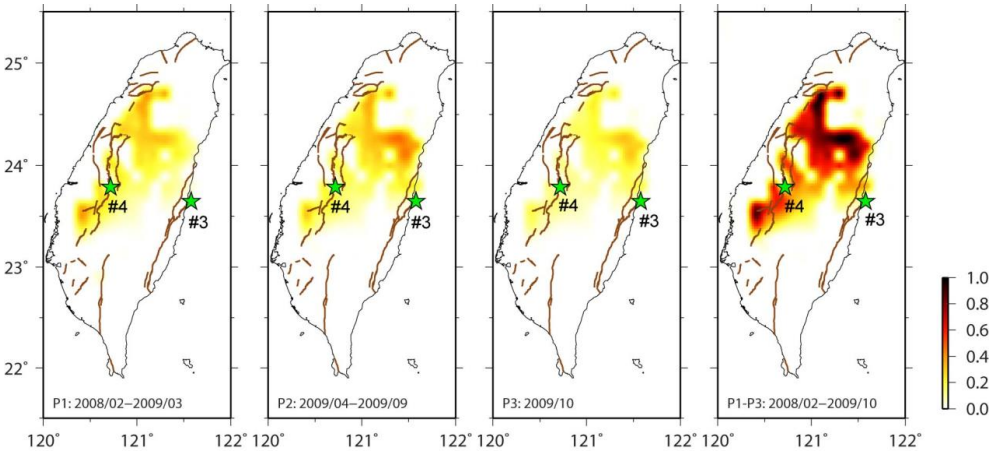

Figure 6: The summed seismic activation map for different period of the seismic activation stage prior to event No. 4. Stars represent the locations of the event Nos. 3 and 4. The active faults (thick lines) identified by the Central Geological Survey of Taiwan are also shown.

4.2 Implication of Tectonic Setting

Several major active faults in southern Taiwan were identified, and most of them were dominated by thrust movement. Some strike-slip structures, e.g. the Zuochen and Hsinhua fault, played as the transfer structures between those thrust faults (Ching et al., 2011; Deffontaines et al., 1994, 1997; Rau et al., 2012). These transfer structures develop around 23°N, where is the northern limit of the Wadati-Benioff zone (Kao et al., 2000) and close to the seismicity boundary indicated in Figs. 2 and 4. Geodetic data

https://doi.org/10.5194/nhess-2022-114
Preprint. Discussion started: 31 March 2022


Natural Hazards and Earth System Sciences
Discussions

229 revealed the various rate and orientation horizontal shortening with rapid uplift rates in
230 the southern Taiwan (Fig. 1), which might be caused by the underplating beneath the
231 Central Range sustain crustal thickening and exhumation (Simoes et al., 2007). The
232 seismicity in southern Central Range is active but showing significant heterogeneity in
233 faulting types (Chen et al., 2017), and high b-values suggest the predominance of small
234 earthquakes in this region (Fig. 2 and red dots in Fig. 5a). Wen et al. (2016) revealed
235 the seismicity decrease in the southern Central Range prior to the 2010 Jiashian
236 earthquake (i.e., event No. 5). The seismicity rate change can be considered as a proxy
237 for the stress state change (Dieterich, 1994; Dieterich et al., 2000), and both variations
238 in Coulomb stress and seismicity rate play important roles contributing to the nucleation
239 process of impending earthquakes (Wen et al., 2016). Since this high b-value region in
240 southern Central Range is observed seismicity decrease ($2.5<M<4.5$ events) before the
241 occurrence of Q-type events, it can be an indicator of stress change.

242 Many devastating earthquakes with surface rupture occurred in this region,
243 including the 1935 M 7.1 Hsinchu-Taichung earthquake, the 1951 Longitudinal Valley
244 earthquake sequence and the 1999 Chi-Chi earthquake (Lee et al., 2007; Chen et al.,
245 2008; Lin et al., 2013). Hsu et al. (2009) derived the consistent orientations of principal
246 strain-rate and crust stress axes in central Taiwan, which implies that faulting style
247 corresponds to stress buildup accumulating from the interseismic loading. They also
248 pointed out that, for the central Taiwan, the small events tend to surround the locked
249 fault zone, where the major earthquakes might occur, during the interseismic period.
250 The 1999 Chi-Chi earthquake is such case ruptured the area near the end of décollement
251 with a high contraction rate (Dominguez et al., 2003; Hsu et al., 2003; 2009). In addition,
252 similar with the 1999 Chi-Chi earthquake, the A-type events occurred on the low b-
253 value area surrounded by small and active events. Chen and Wu (2006) derived the

https://doi.org/10.5194/nhess-2022-114
Preprint. Discussion started: 31 March 2022

temporal RTL function of the 1999 Chi-Chi earthquake showing similar pattern to the A-type events with the activation stage prior to the mainshock. Furthermore, Wu (2006) calculated the seismic activation map of 1999 Chi-Chi event, and the author also found that the 1999 Chi-Chi mainshock occurred on the edge of the seismic activation area, where is a low b-value region. This is similar with the seismic activation maps of A-type events, which display the hot-spot pattern contracting within the low b-value area (Fig.s 2 and 4). The nucleation of A-type mainshock can be attributed to the perturbation of background seismicity (3<M<5 events) by the stress state change (Dieterich, 1994; Dieterich et al., 2000).

The cumulative frequency distributions of long-term seismicity in Fig. 5 reveal the b-value of 0.8-1.0 around these eight events, which consist with the pattern shown in Fig. 3. However, the cumulative frequency distributions of long-term seismicity exhibit different trends of magnitude larger than 4.5 for two type events that the seismicity for M>4.5 events is lower in area around Q-type event but higher in area around A-type event. Event Nos. 1, 2, 3 and 7, occurred in eastern Taiwan with averaged GPS velocity of about 60 mm/yr (Fig. 1), and the cumulative frequency distributions of long-term seismicity display the high intercept (Fig. 5). This rapid convergence rate roughly remains in the west part of southern Taiwan, which indicates that only few shortening is consumed through east to west in the southern Taiwan. This corresponds to the active seismicity of small earthquakes as revealed by the high intercept of the cumulative frequency distributions of long-term seismicity for event Nos. 1, 2, 5 and 8 (Fig. 5). Therefore, the quiescence of 2.5<M<4.5 activity contributes to accumulate the tectonic stress for preparing the occurrence of the Q-type event. On the other hand, the shortening rate is obviously consumed in the mountain area of central Taiwan. Therefore, the lowest intercept of the cumulative frequency distributions of long-term

https://doi.org/10.5194/nhess-2022-114
Preprint. Discussion started: 31 March 2022

seismicity for event No. 4 (Fig. 5) reflects the slow GPS velocity and low seismicity in the west part of the central Taiwan (Fig. 1). Tectonic stress accumulating from the interseismic loading with the perturbation of the accelerating activity of 3<M<5 events would promote the nucleation process of the A-type event.

5. Conclusion

Through the statistical analyses of recent large earthquakes occurred in Taiwan, we summary various temporal and spatial seismicity patterns prior to the earthquakes nucleating in different region of Taiwan:

- Q-type events occurred in southern Taiwan, with the northern boundary of 23.2°N, and experienced seismic quiescence stage prior to the mainshock. Seismicity decrease of 2.5<M<4.5 events in the high b-value southern Central Range could be an indicator of stress change related to the preparation process of such type event.
- A-type events occurred in central Taiwan and experienced seismic activation stage prior to the mainshock, which nucleated on the edge of the seismic activation area. We should pay attention when accelerating seismicity of 3<M<5 events appears within the low b-value area.

Our results reveal that the spatiotemporial seismicity variations during the preparation process of impending earthquakes would display distinctive pattern corresponding to the tectonic setting. However, it is not so clear about the mechanisms causing these different phenomena, further study is still needed.

https://doi.org/10.5194/nhess-2022-114
Preprint. Discussion started: 31 March 2022

Data Availability : The seismic data is available in the Geophysical Database Management System (GDMS, https://gdms.cwb.gov.tw/). A Chinese manual for data access from the GDMS is on the website.

Author contributions: Conceptualisation, YYW, CCC; Investigation, YYW, WTL; Validation, Formal analysis, Writing - original draft preparation, YYW; Writing - review & editing, YYW, CCC, SW.

Competing interests: The authors declare no conflicts of interest.

Acknowledgments: We thank Central Weather Bureau (CWB) of Taiwan for providing seismic data. This research was supported by the Ministry of Science and Technology in Taiwan with grant: MOST 110-2116-M-194-018. The Taiwan Earthquake Center (TEC) contribution number for this article is ****.

https://doi.org/10.5194/nhess-2022-114
Preprint. Discussion started: 31 March 2022


Natural Hazards and Earth System Sciences Discussions

References:

Chan, C.H., Wu, Y.M., Tseng, T.L., Lin, T.L., and Chen, C.C.: Spatial and temporal evolution of b-values before large earthquakes in Taiwan. *Tectonophysics*, **532**, 215-222, 2012.

Chen, C.-C., Rundle, J.B., Holliday, J.R., Nanjo, K.Z., Turcitte, D.L., Li, S.C., and Tiampo, K. F.: The 1999 Chi-Chi, Taiwan, earthquake as a typical example of seismic activation and quiescence. *Geophys. Res. Lett*., **32**(22), L22315, doi:10.1029/2005GL023991, 2005.

Chen, C.C., and Wu, Y.X.: An improved region–time–length algorithm applied to the 1999 Chi-Chi, Taiwan earthquake. *Geophys. J. Int.*, **166**, 1144-1147, doi 10.1111/j.1365-246X.2006.02975.x, 2006.

Chen, J.S., Ching, K.E., Rau, R.J., Hu, J.C., Cheng, K.C., Chang, W.L., Chuang, R.Y., Chen, C.L., and Chen, H.C.: Surface deformation in Taiwan during 2002-2017 determined from GNSS and precise leveling measurements. Central Geological Survey Special Publication, 33, 157-178, 2018. (in Chinese with English abstract)

Chen, K.H., Toda, S., and Rau, R.J.: A leaping, triggered sequence along a segmented fault: the 1951 Hualien – Taitung earthquake sequence in eastern Taiwan. *J. Geophys. Res*., **113**, B02304, doi:10.1029/2007JB005048, 2008.

Chen, S.K., Wu, Y.M., Hsu, Y.J., and Chan, Y.C.: Current crustal deformation reassessed by cGPS strain-rate estimation and focal mechanism stress inversion. *Geophys. J. Int.*, **210**, 228–239. https://doi.org/10.1093/gji/ggx165, 2017.

Ching, K.E., Johnson, K.M., Rau, R.J., Chuang, R.Y., Kuo, L.C., and Leu, P.L.: Inferred fault geometry and slip distribution of the 2010 Jiashian, Taiwan, earthquake is consistent with a thick-skinned deformation model. *Earth Planet. Sci. Lett.*, EPSL-S-10-00445, doi:10.1016/j.epsl.2010.10.021, 2011.

https://doi.org/10.5194/nhess-2022-114
Preprint. Discussion started: 31 March 2022


Natural Hazards and Earth System Sciences Discussions

343 Deffontaines, B., Lee, J.-C., Angelier, J., Carvalho, J., and Rudant, J.-P.: New
344 geomorphic data on the active Taiwan orogen: a multisource approach. *J. Geophys.*
345 *Res.*, **99**, 20243–20266, 1994.
346 Deffontaines, B., Lacombe, O., Angelier, J., Mouthereau, F., Lee, C.T., Deramond, J.,
347 Lee, J.F., Yu, M.S., and Liu, P.M.: Quaternary transfer faulting in Taiwan
348 Foothills: evidence from a multisource approach. *Tectonophysics*, **274**, 61–82,
349 1997.
350 Dieterich, J. H.: A constitutive law for rate of earthquake production and its application
351 to earthquake clustering. *J. Geophys. Res*., **99** (18), 2601-2618, 1994.
352 Dieterich, J., Cayol, V., and Okubo, P.: The use of earthquake rate changes as a stress
353 meter at Kilauea volcano. *Nature*, **408**, 457–460, 2000.
354 Dominguez, S., Avouac, J.P., and Michel, R.: Horizontal coseismic deformation of the
355 1999 Chi-Chi earthquake measured from SPOT satellite images: implications for
356 the seismic cycle along the western foothills of central Taiwan. *J. Geophys. Res*.,
357 **108**, doi:10.1029/2001JB000951, 2003.
358 Gardner, J. K., and Knopoff, L.: Is the sequence of earthquakes in Southern California,
359 with aftershocks removed, Poissonian?. *Bull. Seis. Soc. Am*., **64**(5), 1363-1367,
360 1974.
361 Hsu, Y.J., Simons, M., Yu, S.B., Kuo, L.C., and Chen, H.Y.: A two-dimensional
362 dislocation model for interseismic deformation of the Taiwan mountain belt. *Earth*
363 *Planet. Sci. Lett.*, **211**, 287–294, 2003.
364 Hsu, Y.J., Yu, S.B., Simons, M., Kuo, L.C., and Chen, H.Y.: Interseismic crustal
365 deformation in the Taiwan plate boundary zone revealed by GPS observations,
366 seismicity, and earthquake focal mechanisms. *Tectonophysics*, **479**, 4–18.
367 https://doi.org/10.1016/j.tecto.2008.11.016, 2009.

https://doi.org/10.5194/nhess-2022-114
Preprint. Discussion started: 31 March 2022


Natural Hazards and Earth System Sciences Discussions

368 Huang, Q., and Ding, X.: Spatiotemporal variations of seismic quiescence prior to the
369 2011 M 9.0 Tohoku earthquake revealed by an improved Region-Time-Length
370 algorithm. *Bull. Seismol. Soc. Am.,* **102**(4), 1878-1883, doi: 10.1785/0120110343,
371 2012.
372 Huang, Q., Sobolev, G.A., and Nagao, T.: Characteristics of the seismic quiescence and
373 activation patterns before the M=7.2 Kobe earthquake. *Tectonophysics,* **337**, 99-
374 116, 2001.
375 Kao, H., Huang, G.C., and Liu, C.S.: Transition from oblique subduction to collision in
376 the northern Luzon arc-Taiwan region: Constraints from bathymetry and seismic
377 observations. *J. Geophys. Res*., **105**, 3059-3079, 2000.
378 Kasahara, K.: Earthquake Mechanics, *Cambridge Univ. Press., Cambridge*, 248 pp.,
379 1981.
380 Lee, S.J., Chen, H.W., and Ma, K.F.: Strong Ground Motion Simulation of the 1999
381 Chi-Chi, Taiwan, Earthquake from a Realistic 3D Source and Crustal Structure. *J.*
382 *Geophys. Res.*, **112**, B06307, doi: 10.1029/2006JB004615, 2007.
383 Lin, D.-H., Chen, H., Rau, R.-J., and Hu, J.-C.: The role of a hidden fault in stress
384 triggering: Stress interactions within the 1935 Mw 7.1 Hsinchu–Taichung
385 earthquake sequence in central Taiwan, Tectonophysics. 37-52, doi:
386 10.1016/j.tecto.2013.04.022, 2013.
387 Lu, W. T.: Seismicity Changes Prior to the M>6 Earthquakes in Taiwan During 1993
388 to 2016 - an Approach of the RTL Algorithm. M.Sc. thesis, National Chung Cheng
389 University, Taiwan, p 66, 2017. (in Chinese with English abstract)
390 Mignan, A., and Giovambattista, R. Di: Relationship between accelerating seismicity
391 and quiescence, two precursors to large earthquakes. *Geophys. Res. Lett.*, **35**,
392 L15306, doi:10.1029/2008GL035024, 2008.

https://doi.org/10.5194/nhess-2022-114
Preprint. Discussion started: 31 March 2022


Natural Hazards and Earth System Sciences Discussions

393 Rau, R.J., Lee, J.C., Ching, K.E., Lee, Y.H., Byrne, T.B., and Chen, R.Y.: Subduction-
394 continent collision in southwestern Taiwan and the 2010 Jiashian earthquake
395 sequence. *Tectonophysics*, **578**, 107-116, doi:10.1016/j.tecto.2011.09.013, 2012.
396 Rundle, J.B., Turcotte, D.L., Shcherbakov, R., Klein, W., and Sammis, C.: Statistical
397 physics approach to understanding the multiscale dynamics of earthquake fault
398 systems. *Rev. Geophys*., **41**(4), 1019, doi:10.1029/2003RG000135, 2003.
399 Simoes, M., Avouac, J.P., Beyssac, O., Goffe, B., Farley, K.A., and Chen, Y.G.:
400 Mountain building in Taiwan: a thermokinematic model. *J. Geophys. Res*., **112**.
401 doi:10.1029/2006JB004824, 2007.
402 Shyu, J.B.H., Sieh, K., Chen, Y.-G., and Liu, C.-S.: Neotectonic architecture of Taiwan
403 and its implications for future large earthquakes. *J. Geophys. Res.*, **110**, p. B08402,
404 doi: 10.1029/2004JB003251, 2005.
405 Sobolev, G.A., and Tyupkin, Y.S.: Low-seismicity precursors of large earthquakes in
406 Kamchatka. *Volc. Seismol.*, **18**, 433-446, 1997.
407 Sobolev, G.A., and Tyupkin, Y.S.: Precursory phases, seismicity precursors, and
408 earthquake prediction in Kamchatka. *Volc. Seismol.*, **20**, 615-627, 1999.
409 Suppe, J.: Kinematics of arc-continent collision, flipping of subduction, and backarc
410 spreading near Taiwan. *Mem. Geol. Soc. China*, 21–33, 1984.
411 Wang, J.H.:. The Taiwan Telemetered Seismographic Network. *Phys. Earth Planet.*
412 *Inter*., **58**, 9–18, 1989
413 Wang, J.H., Chen, K.C., and Lee, T.Q.: Depth distribution of shallow earthquakes in
414 Taiwan. *J. Geol. Soc. China*, **37**, 125–142, 1994.
415 Wen, Y.-Y., Chen, C.-C., Wu, Y.-H., Chan, C.-H., Wang, Y.-J., and Yeh, Y.-L.:
416 Spatiotemporal investigation of seismicity and Coulomb stress variations prior to

https://doi.org/10.5194/nhess-2022-114
Preprint. Discussion started: 31 March 2022


Natural Hazards and Earth System Sciences
Discussions

the 2010 ML 6.4 Jiashian, Taiwan earthquake. *Geophys. Res. Lett.*, **43**, doi:10.1002/2016GL070633, 2016.

Wen, Y.-Y., and Chen, C.-C.: Seismicity variations prior to the 2016 ML 6.6 Meinong, Taiwan earthquake. *Terr. Atmos. Ocean. Sci.*,**28**, 737-742, doi: 10.3319/TAO.2016.12.05.01, 2017.

Wu, Y. H.: An improved region–time–length algorithm applied to the 1999 Chi-Chi, Taiwan earthquake. M.Sc. thesis, National Central University, Taiwan, p 115, 2006. (in Chinese with English abstract)

Wu, Y.M., Hsu, Y.J., Chang, C.H., Teng, L.S., and Nakamura, M.: Temporal and spatial variation of stress field in Taiwan from 1991 to 2007: Insights from comprehensive first motion focalmechanism catalog. *Earth Planet. Sci. Lett.*, **298**, 306–316. https://doi.org/10.1016/j.epsl.2010.07.047, 2010.

Wyss, M., and Stefansson, R.: Nucleation points of recent mainshocks in Southern Iceland, mapped by b-values. *Bull. Seismol. Soc. Am.*, **96**, 599–608, 2006.

Yu, S.B., Chen, H.Y., and Kuo, L.C.: Velocity field of GPS stations in the Taiwan area. Tectonophysics. 274(1-3), 41–59. https://doi.org/10.1016/S0040-1951(96)00297-1, 1997.